


# Extending microwave-frequency electric-field detection through single transmission peak method

Qing Liu(刘青), Jin-Zhan Chen(陈进湛), He Wang(王赫), Jie Zhang(张杰), Wei-Min Ruan(阮伟民), Guo-Zhu Wu(伍国柱), Shun-Yuan Zheng(郑顺元), Jing-Ting Luo(罗景庭), and Zhen-Fei Song(宋振飞)

**Citation:**Chin. Phys. B, 2024, 33 (**5**): 054203. DOI: 10.1088/1674-1056/ad2a6f
Journal homepage: http://cpb.iphy.ac.cn; http://iopscience.iop.org/cpb

**What follows is a list of articles you may be interested in**

---

## Dependence of Rydberg-atom-based sensor performance on different Rydberg atom populations in one atomic-vapor cell

Bo Wu(武博), Jiawei Yao(姚佳伟), Fengchuan Wu(吴逢川), Qiang An(安强), and Yunqi Fu(付云起)
Chin. Phys. B, 2024, 33 (**2**): 024205. DOI: 10.1088/1674-1056/ad0b04

## Light manipulation by dual channel storage in ultra-cold Rydberg medium

Xue-Dong Tian(田雪冬), Zi-Jiao Jing(景梓骄), Feng-Zhen Lv(吕凤珍),Qian-Qian Bao(鲍倩倩), and Yi-Mou Liu(刘一谋)
Chin. Phys. B, 2023, 32 (**4**): 044205. DOI: 10.1088/1674-1056/ac946c

## Monte Carlo simulations of electromagnetically induced transparency in a square lattice of Rydberg atoms

Shang-Yu Zhai(翟尚宇) and Jin-Hui Wu(吴金辉)
Chin. Phys. B, 2021, 30 (**7**): 074206. DOI: 10.1088/1674-1056/abd75a

## Nonlinear spectroscopy of three-photon excitation of cesium Rydberg atoms in vapor cell

Jiabei Fan(樊佳蓓), Yunhui He(何云辉), Yuechun Jiao(焦月春), Liping Hao(郝丽萍), Jianming Zhao(赵建明), and Suotang Jia(贾锁堂)
Chin. Phys. B, 2021, 30 (**3**): 034207. DOI: 10.1088/1674-1056/abca25

## A sensitive detection of high Rydberg atom with large dipole moment

Shan-Shan Zhang(张珊珊), Hong Cheng(成红), Pei-Pei Xin(辛培培), Han-Mu Wang(王汉睦), Zi-Shan Xu(徐子珊), Hong-Ping Liu(刘红平)
Chin. Phys. B, 2018, 27 (**7**): 074207. DOI: 10.1088/1674-1056/27/7/074207

---

# Extending microwave-frequency electric-field detection through single transmission peak method

Qing Liu(刘青)[1,2], Jin-Zhan Chen(陈进湛)[2], He Wang(王赫)[2], Jie Zhang(张杰)[2], Wei-Min Ruan(阮伟民)[2], Guo-Zhu Wu(伍国柱)[2], Shun-Yuan Zheng(郑顺元)[2], Jing-Ting Luo(罗景庭)[1], and Zhen-Fei Song(宋振飞)[2,3,†]

[1] *College of Physics and Optoelectronic Engineering, Shenzhen University, Shenzhen* 518060, *China*
[2] *Shenzhen Institute for Technology Innovation, National Institute of Metrology, Shenzhen* 518107, *China*
[3] *Center for Advanced Measurement Science, National Institute of Metrology, Beijing* 100029, *China*

(Received 9 December 2023; revised manuscript received 31 January 2024; accepted manuscript online 19 February 2024)

The strength of microwave (MW) electric field can be observed with high precision by using the standard electromagnetically induced transparency and Aulter–Towns (EIT-AT) technique, when its frequency is resonant or nearly-resonant with the Rydberg transition frequency. As the detuning of MW field increases, one of the transmission peaks (single peak) is easier to measure due to its increased amplitude. It can be found that the central symmetry point of the two transmission peaks $f_{1/2}$ is only related to the detuning of MW field $\Delta_{\rm MW}$ and central symmetry point $f_0$ of resonant MW field, satisfying the relation $f_{1/2} = \Delta_{\rm MW}/2 + f_0$. Thus, we demonstrate a single transmission peak method that the MW E-field can be determined by interval between the position of single peak and $f_{1/2}$. We use this method to measure continuous frequencies in a band from $-200$ MHz to 200 MHz of the MW field. The experimental results and theoretical analysis are presented to describe the effectiveness of this method. For 50 MHz $< \Delta_{\rm MW} <$ 200 MHz, this method solves the problem that the AT splitting cannot be measured by using the standard EIT-AT techniques or multiple atomic-level Rydberg atom schemes.

**Keywords:** microwave electric field, Rydberg atom, electromagnetically induced transparency (EIT), Aulter–Towns splitting

**PACS:** 42.50.Gy, 32.80.Ee, 84.40.–x **DOI:** 10.1088/1674-1056/ad2a6f

## 1. Introduction

Rydberg atoms are the highly excited atoms with the principal quantum number $n > 10$, which are sensitive to external fields due to the large dipole moments and polarizabilities.[1,2] Based on the Rydberg atomic system, in recent years, many researchers have demonstrated a new method of measuring the electric ($E$) field by using the electromagnetically induced transparency (EIT) and Autler–Townes (AT) splitting, which can be directly traced to the International System of Units (SI).[3–10] The EIT is a typical quantum interference effect that the atoms become transparent to the probe laser transmission in the presence of strongly coupled light. When the microwave (MW) $E$-field that resonates with the Rydberg atomic transition frequency is applied, the EIT spectrum will split proportionally to the power of the field. By measuring the splitting $\Delta f_{\rm m}$, the MW $E$-field can be directly obtained from

$$|E| = 2\pi \frac{\hbar}{\wp} D \Delta f_{\rm m}. \tag{1}$$

Here, $\hbar$ is Planck's constant providing a link to SI traceability, $\wp$ is the atomic dipole moment of the MW transition, $D$ represents a residual Doppler parameter, where $D = \lambda_{\rm p}/\lambda_{\rm c}$ and $D = 1$ corresponding to the scanning the probe and coupling light, respectively,[5,11,12] with $\lambda_{\rm p}$ and $\lambda_{\rm c}$ being the probe laser wavelength and the coupling laser wavelength, respectively.

The EIT-AT technology has shown high precision and sensitivity in measurement, which drives the development of many application fields, including SI-traceable standards for $E$-field strength,[3,13–17] microwave imaging,[7,18,19] microwave sensing and communication,[20–24] and polarization measurements.[25] However, the MW $E$-field can be measured accurately when its frequency is resonant or nearly-resonant with the Rydberg transition frequency, which limits the practical application of the Rydberg EIT technology in many scenarios. Several schemes for studying continuous frequency measurements have been proposed.[4,12,26–28] Simons *et al.* studied the continuous measurement of nearly-resonant microwave electric field (±30 MHz) by using an MW detuning method.[4] According to the atomic superheterodyne method, Cui *et al.* used an auxiliary microwave field to extend the bandwidth sensitivity for detecting microwave fields tuning frequency up to 100 MHz from resonance with the Rydberg-Rydberg transition.[12] Adding another MW $E$-field coupled with an adjacent Rydberg transition, Simons *et al.* detected the continuous frequencies through changing the strength or the frequency of MW $E$-field. Although the continuous tuning frequency range exceeding 1 GHz was achieved, they did not obtain the corresponding electric field strength. In addition, the AT splitting was not resolvable within $\Delta_{\rm MW} < 200$ MHz (the detuning of MW $E$-field) by using this method.[26]

Unlike the previous off-resonant scheme, in this paper, we propose a method to extend frequency bands for measuring MW $E$-field. When an MW field is detuned from its resonant

†Corresponding author. E-mail: songzf@nim.ac.cn

© 2024 Chinese Physical Society and IOP Publishing Ltd 

transition frequency, the peak value of one of the transmission peaks for AT splitting will increase. It is found from theoretical analysis that the center $f_{1/2}$ of the asymmetric AT-splitting is only related to $\Delta_{\rm MW}$ and the center $f_0$ of AT splitting at zero MW-detuning, which are discussed in detail later in this work. We propose a single transmission peak method that can perform the non-resonant measurement of the MW field by using single transmission peak and $f_{1/2}$. The measurement of MW $E$-field for non-resonant frequencies is simplified without an additional MW $E$-field by using this method, thereby directly measuring the position of higher transmission peak and $f_0$. In this work, we achieve measurement in a frequency band ranging from $-200$ MHz to $+200$ MHz, which breaks through the limitations that the AT splitting cannot be observed by using the standard EIT-AT techniques[3] or multiple atomic-level Rydberg-atom schemes,[26] for the detuning of MW $E$-field frequency ranging from 50 MHz to 200 MHz.

## 2. Experiment setup

The Rydberg-EIT experiments are performed in a rubidium atomic vapor cell at a controlled temperature of 299.15 K. The energy-level diagram and a schematic of the experimental setup are shown in Fig. 1. Figure 1(a) shows that the levels $|1\rangle$, $|2\rangle$, $|3\rangle$, and $|4\rangle$ correspond to the $^{87}$Rb ground states $5S_{1/2}$, excited state $5P_{3/2}$, and two Rydberg states $50D_{5/2}$ and $51P_{3/2}$, respectively. The probe light with wavelength 780 nm is generated by a tunable external-cavity semiconductor laser (DL-Pro, Toptica) and the coupling light with wavelength 480 nm is produced by a frequency-doubled semiconductor laser (TA-SHG-Pro, Toptica). The probe laser of 780 nm is locked on the saturation absorption spectrum of $^{87}$Rb at the crossover frequency between $5S_{1/2}(F=2)\rightarrow 5P_{3/2}(F'=2)$ and $5S_{1/2}(F=2)\rightarrow 5P_{3/2}(F'=3)$, and 211.79 MHz is shifted to the resonance transition $5S_{1/2}(F=2)\rightarrow 5P_{3/2}(F'=3)$ by using a double-passed acoustic-optical modulator (AOM). The full width at half-maximum (FWHM) and power of probe laser are 160 μm and 80 μW. To produce the Rydberg states $50D_{5/2}$ of $^{87}$Rb, a 480-nm counter-propagating coupling laser with a power of 120 mW is used, and focused to an FWHM of 260 μm.

The method of locking the probe beam and detecting its transmission while modulating the coupling laser with a square wave removes the Doppler background and isolates the EIT signal. The probe light and coupling light collinearly counter-propagate through the center of the 50-mm-long and 20-mm-diameter cylindrical glass vapor containing ($^{87}$Rb) atoms as indicated in Fig. 1(b). An RF $E$-field with a frequency of 17.04 GHz is applied to coupled Rydberg states $50D_{5/2}$ and $51P_{3/2}$ by using a horn antenna placed 37.60 cm away from the vapor cell. The signal of weak probe laser is detected with a photodiode (PD).

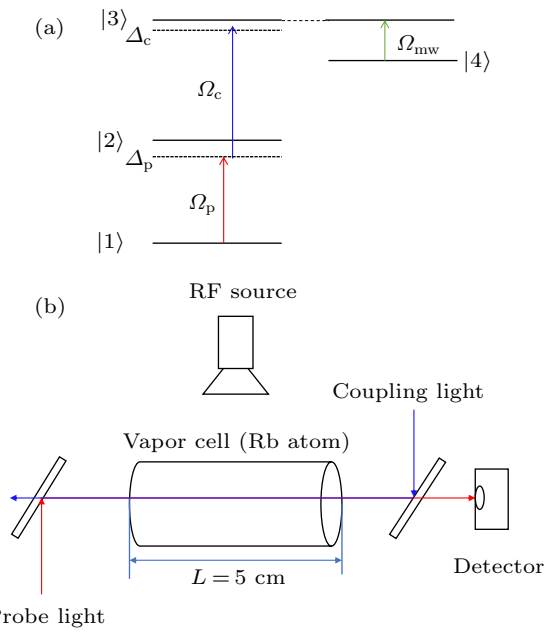



**Fig. 1.** (a) Four-level atomic energy diagram consisting of a ground state $|1\rangle$, excited state $|2\rangle$, and two Rydberg states $|3\rangle$ and $|4\rangle$, with a 780-nm probe light driving transition $|1\rangle = |5S_{1/2}F=2\rangle \rightarrow |2\rangle = |5P_{3/2},F'=3\rangle$, a 480-nm coupling light driving transition $|2\rangle = |5P_{3/2},F'=3\rangle \rightarrow |3\rangle = |50D_{3/2}\rangle$, and an applied RF electric field coupling the transition $|3\rangle = |50D_{5/2}\rangle \rightarrow |4\rangle = |51P_{3/2}\rangle$. (b) Schematic diagram of experimental setup, with probe light (red) overlapping the counter propagating coupling light (blue), and the applied RF field propagating transverse to the optical beam in the vapor cell.

## 3. Theoretical method

The atomic motion of the laser-driven system can be described by using the master equation

$$\dot{\rho} = -\frac{\mathrm{i}}{\hbar}[H_{\rm int},\rho] + \Gamma(\rho) \tag{2}$$

for the density matrix operator. In Eq. (2), $H_{\rm int}$ is Hamiltonian and can be expressed as

$$H_{\rm int} = H_0 + H_{\rm L}, \tag{3}$$

with $H_0$ being Hamiltonian of free atom, $H_{\rm L}$ represents the interaction between light field and atom, and $\Gamma(\rho)$ denotes the operator describing the decay process in the atom.

In this work, we investigate a four-level system composed of the ground state $|1\rangle$, excited states $|2\rangle$, and two Rydberg states $|3\rangle$ and $|4\rangle$ as shown in Fig. 1(a). In order to more clearly describe the interaction between atoms and light fields, the Hamiltonian of this four-level system can be described as

$$H_{\rm int} = \frac{\hbar}{2}\begin{pmatrix} 0 & \Omega_{\rm p} & 0 & 0 \\ \Omega_{\rm p} & -2\Delta_{\rm p} & \Omega_{\rm c} & 0 \\ 0 & \Omega_{\rm c} & -2(\Delta_{\rm p}+\Delta_{\rm c}) & \Omega_{\rm MW} \\ 0 & 0 & \Omega_{\rm MW} & -2(\Delta_{\rm p}+\Delta_{\rm c}-\Delta_{\rm MW}) \end{pmatrix} \tag{4}$$

in the rotating wave representation.[9,26,29–31] Here, $\Omega_{\rm p,c,MW}$ are Rabi frequencies associated with the probe laser, coupling laser, and the MW source, respectively. $\Delta_{\rm p} = w_{12} - w_{\rm p}$, $\Delta_{\rm c} = w_{23} - w_{\rm c}$, and $\Delta_{\rm MW} = w_{34} - w_{\rm MW}$ are detuning of the probe, coupling, and MW $E$-field, respectively, where $w_{12}$, $w_{23}$, and $w_{34}$ are the resonant frequencies of transition $|1\rangle \to |2\rangle$, $|2\rangle \to |3\rangle$, and $|3\rangle \to |4\rangle$, respectively, $w_{\rm p,c,MW}$ are frequencies of probe field, coupling field, and the MW field, respectively.

The $\Gamma(\rho)$ can be expressed as

$$\Gamma(\rho) = \begin{pmatrix} \Gamma_2\rho_{22} & -\gamma_{12}\rho_{12} & -\gamma_{13}\rho_{13} & -\gamma_{14}\rho_{14} \\ -\gamma_{21}\rho_{21} & -\Gamma_2\rho_{22}+\Gamma_3\rho_{33} & -\gamma_{23}\rho_{23} & -\gamma_{24}\rho_{24} \\ -\gamma_{31}\rho_{31} & -\gamma_{32}\rho_{32} & -\Gamma_3\rho_{33} & -\gamma_{34}\rho_{34} \\ -\gamma_{41}\rho_{41} & -\gamma_{42}\rho_{42} & -\gamma_{43}\rho_{43} & \Gamma_3\rho_{33}-\Gamma_4\rho_{44} \end{pmatrix} \tag{5}$$

for the four-level system. Here $\gamma_{ij} = (\Gamma_i + \Gamma_j)/2$, with $\Gamma_{i,j}$ being the decay rates.

Under the condition of the weak probe limit, the steady-state solution for Eq. (2) can be exactly described as follows:

$$\rho_{21} = -\frac{\mathrm{i}\Omega_{\rm p}/2}{\gamma_{21} - \mathrm{i}\Delta_{\rm p} + \dfrac{\Omega_{\rm c}^2/4}{\gamma_{31} - \mathrm{i}(\Delta_{\rm p}+\Delta_{\rm c}) + \dfrac{\Omega_{\rm MW}^2/4}{\gamma_{41} - \mathrm{i}(\Delta_{\rm p}+\Delta_{\rm c}-\Delta_{\rm MW})}}}. \tag{6}$$

Considering the Doppler broadening effect, the detuning of probe and coupling beam is modified as

$$\begin{aligned} &\Delta_{\rm p}' = \Delta_{\rm p} - \frac{2\pi}{\lambda_{\rm p}}v, \quad \Delta_{\rm c}' = \Delta_{\rm c} + \frac{2\pi}{\lambda_{\rm c}}v, \\ &\Delta_{\rm MW}' = \Delta_{\rm MW} - \frac{2\pi}{\lambda_{\rm MW}}v, \end{aligned} \tag{7}$$

where $v$ is the velocity of atom. The absorption coefficient for probe beam can be given by

$$\begin{aligned} \alpha = &\frac{2\pi}{\lambda_{\rm p}}\,\mathrm{Im}\left(\frac{2N_0\wp_{12}^2}{\varepsilon_0\hbar\Omega_{\rm p}}\frac{1}{u\sqrt{\pi}}\right. \\ &\left.\times\int_{-3u}^{3u}\rho_{21}(\Delta_{\rm p}', \Delta_{\rm c}', \Delta_{\rm MW}')\,\mathrm{e}^{-v^2/u^2}\,\mathrm{d}v\right), \end{aligned} \tag{8}$$

with considering the Doppler broadening effect and normalized one-dimensional Maxwell velocity distribution. Here, $u = \sqrt{2k_{\rm B}T/m}$ represents the most probable speed of atoms, $\wp_{12} = 2.04ea_0$ denotes the electric dipole matrix element for transition $|1\rangle \to |2\rangle$. $N_0$ is the total atomic density in the cell.[32] The transmission of probe laser is given by

$$T = \exp(-\alpha L). \tag{9}$$

The transmission spectrum can be obtained by numerically solving Eq. (9).

## 4. Results and discussion

In the presence of the coupling laser as shown by the black line in Fig. 2, the EIT windows of atom are observed for the probe laser transmission while scanning the couple beam within the frequency range of the detuning from −100 MHz to 100 MHz. According to Eqs. (2)–(9), when the Rabi frequency of MW $E$-field is zero, the transmission coefficient can be obtained within the frequency range of $\Delta_{\rm c} = -100$ MHz–+100 MHz by using the numerical method, which indicates the transmission characteristics of probe light. The corresponding transmission spectrum is shown by the red dash-dotted line in Fig. 2, which is in agreement with that of experimental signal. It can be seen from Fig. 2 that the range of the calculated transmission coefficient is 0.68–1.00, which relates to the physical variables, such as detuning and atomic density. A more detailed description about the influence of those physical variables can be found in Ref. [33]. Additionally, the interval 92.44 MHz between two transmission peaks corresponds to the frequency interval of Rydberg states $|50\mathrm{D}_{5/2}\rangle$ and $|50\mathrm{D}_{3/2}\rangle$, which is consistent with the theoretical value 92.73 MHz obtained by the ARC (Alkali.ne Rydberg Calculator) code.[34]

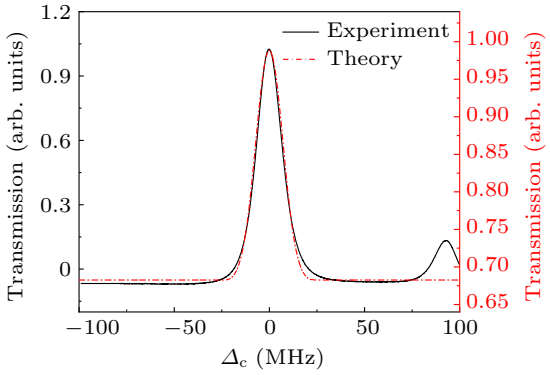



**Fig. 2.** Two-photon EIT spectrum of $^{87}$Rb atoms with black line denoting experimental result, and the red dash-dot line representing theoretical data. It should be noted that the strongest transmission is normalized to one.

The MW $E$-field with a frequency of 17.04 GHz couples two Rydberg states $|50\mathrm{D}_{5/2}\rangle$ and $|51\mathrm{P}_{3/2}\rangle$, resulting in AT splitting. According to Eq. (1), the measurement of AT splitting can be directly obtained the MW $E$-field strength.[26] Figure 3(a) shows the experimental AT spectra with and without the detuning of the MW $E$-field for an SG power level of 0 dBm. Like Fig. 2, the theoretical AT spectra are also obtained by solving Eq. (9) in the detuning frequency range from

$\Delta_c = -100$ MHz to $+100$ MHz, which is shown in Fig. 3(b). The black solid curve represents the AT signal obtained by the MW $E$-field with a resonant frequency of 17.04 GHz. The red dash curve and blue dash curve denote the AT signal generated by the MW $E$-field with a detuning of $\Delta_{MW} = -50$ MHz and $\Delta_{MW} = 50$ MHz, respectively. As shown in the figures, the peak positions of the theoretical AT splitting are consistent with those of the experimental AT splitting for the different detuning values of $\Delta_{MW} = 0$, and $\pm 50$ MHz. We can also see that if the MW frequency detuning is $-50$ MHz, the left peak is lower than that of the right peak. If the MW frequency detuning is 50 MHz, the heights of the two peaks are opposite. In addition, the separation between the two peaks increases with MW detuning increasing.

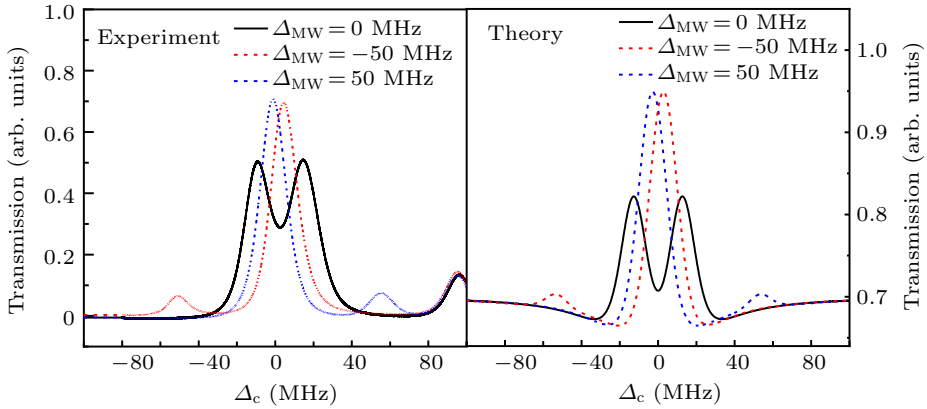



**Fig. 3.** Variations of AT signal with coupling laser detuning $\Delta_c$ for $\Delta_{MW} = 0$ MHz (black line), $-50$ MHz (red dash–dotted line), and $+50$ MHz (blue dash line), showing (a) experimental results and (b) theoretical data from an applied 17.04-GHz microwave (MW) $E$-field for 0 dBm.

As shown in Fig. 3, the asymmetric amplitudes of the peaks illustrate that the AT splitting is difficult to measure when the detuning of MW field ($\Delta_{MW}$) is over $\pm 50$ MHz. Taking $\Delta_{MW} = 50$ MHz for example, we can find that the amplitude of left transmission peak is much greater than that of right one. It is difficult to solve the eigenstates and eigenvalues even in resonant situation for this system. In order to study the influence of MW $E$-field, we simplify the Hamilton as follows:

$$H = \frac{\hbar}{2}\begin{pmatrix} 0 & 0 & 0 & 0 \\ 0 & 0 & 0 & 0 \\ 0 & 0 & 0 & \Omega_{MW} \\ 0 & 0 & \Omega_{MW} & 2\Delta_{MW} \end{pmatrix}. \tag{10}$$

The eigenvalues and eigenvectors of dressed dark states are obtained from the following formulas:

$$\begin{aligned} E_1 &= \frac{\Delta_{MW}}{2} - \frac{\sqrt{\Delta_{MW}^2 + \Omega_{MW}^2}}{2}, \\ E_2 &= \frac{\Delta_{MW}}{2} + \frac{\sqrt{\Delta_{MW}^2 + \Omega_{MW}^2}}{2}, \end{aligned} \tag{11}$$

$$\begin{aligned} |E_1\rangle = \Bigg(0, 0, &\frac{-\Delta_{MW} - \Omega_{MW,\Delta}}{\sqrt{(-\Delta_{MW} - \Omega_{MW,\Delta})^2 + \Omega_{MW}^2}}, \\ &\frac{\Omega_{MW}}{\sqrt{(-\Delta_{MW} - \Omega_{MW,\Delta})^2 + \Omega_{MW}^2}}\Bigg)^{\mathrm{T}}, \end{aligned} \tag{12}$$

$$\begin{aligned} |E_2\rangle = \Bigg(0, 0, &\frac{-\Delta_{MW} + \Omega_{MW,\Delta}}{\sqrt{(-\Delta_{MW} + \Omega_{MW,\Delta})^2 + \Omega_{MW}^2}}, \\ &\frac{\Omega_{MW}}{\sqrt{(-\Delta_{MW} + \Omega_{MW,\Delta})^2 + \Omega_{MW}^2}}\Bigg)^{\mathrm{T}}, \end{aligned} \tag{13}$$

where $\Omega_{MW,\Delta} = \sqrt{\Omega_{MW}^2 + \Delta_{MW}^2}$ represents Rabi frequency with detuned MW field.

According to Eq. (11), the energy level interval equals $\Delta E = E_2 - E_1 = \Omega_{MW,\Delta}$, which is corresponding to the AT splitting as the MW $E$-field is detuned. As shown in Fig. 4, taking the spectrum with microwave frequency detuning of 50 MHz for example, we can obtain the expression $\Delta E/2 = f_{1/2} - E_1 = E_2 - f_{1/2}$, where $f_{1/2}$ represents the center frequency between the transmission peaks, the $E_1$ and $E_2$ can be obtained from Eq. (11).

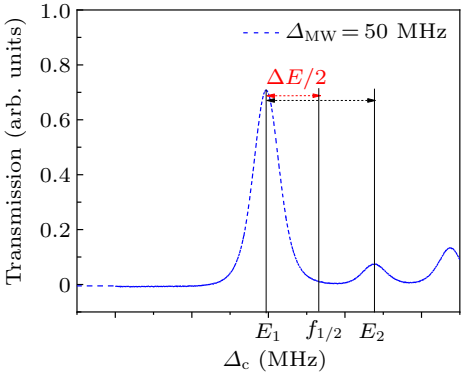



**Fig. 4.** AT signal for SG power level of 0 dBm and $\Delta_{MW} = 50$ MHz, with $E_1$ and $E_2$ denoting eigenvalues, and $f_{1/2}$ representing center frequency.

Thus, the center frequency $f_{1/2}$ can be obtained with

$$f_{1/2} = E_2 - \frac{\Delta E}{2} = \frac{\Delta E}{2} + E_1 = \frac{\Delta_{MW}}{2}. \tag{14}$$

Similarly, it can be inferred that if the center of AT splitting is denoted as $f_0$ with resonant MW field, the following relation

$$f_{1/2} = \frac{\Delta_{MW}}{2} + f_0 \tag{15}$$

is satisfied, as the MW field is detuned away from resonance. Thus, we propose a single transmission peak method that the AT splitting can be determined by the center $f_{1/2}$ of two peaks and the position of the higher transmission peak.

It can be found that as the detuning increases, the movement distances of the transmission peak with increased amplitude is much smaller than that of another peak. For detuning $\Delta_{\rm MW} < 0$, the two transmission peaks of AT splitting move away from the peak with $50D_{3/2}$ that has not affect the measurement results. For detuning $\Delta_{\rm MW} > 0$, the movement of left peak is less than the interval 92.44 MHz between $50D_{3/2}$ and $50D_{5/2}$, thus the influence caused by the $50D_{3/2}$ can be ignored by using the single transmission peak method. For example, the movement of left peak is 15 MHz for the detuning $\Delta_{\rm MW} = 200$ MHz and SG power level of 0 dBm.

As illustrated in Fig. 5, we show the experimental and theoretical results of AT splitting for power values of signal generator (SG) $-6$ dBm, $-3$ dBm, $-2$ dBm, and 0 dBm, respectively. The red squares represent experimental data using standard EIT-AT techniques, which can only be measured within a limited band with detuning of around $\pm 50$ MHz. The frequency range in which an MW field can be observed dramatically increases which is demonstrated by using the single transmission peak method as shown by the black triangle line in Fig. 5. We have achieved continued measurement of frequency from $-200$ MHz to 200 MHz, and the results are consistent with those from the standard EIT-AT method within the detuning range from $-50$ MHz to $+50$ MHz. Theoretically, as shown by the red line in Fig. 5, AT splitting can be obtained by solving the master equation as given by Eq. (2). The green line represents the results obtained from the simulation formula $\Omega_{\rm MW,\Delta} = \sqrt{\Omega_{\rm MW}^2 + \Delta_{\rm MW}^2}$, which is consistent with that by the Lindblad master method and the experimental results.

The AT splitting and MW $E$-field obtained by using standard EIT-AT (double peak) and the single transmission peak method (single peak) are shown in Table 1. We are able to measure AT splitting and $E$-field strength just through measuring the single transmission peak, which is not observed by using standard EIT-AT method. The maximum difference in AT splitting between these two measurements is 2 MHz, the corresponding difference of $E$-field is 0.32 V/m. In the experiment, we locked the coupling light by using wavelength meter (Toptica, WS8), but the frequency fluctuation is about $\pm 2$ MHz, which is the main reason for the difference between the two methods. The accuracy of experimental measurement is expected to be improved by using the higher precision frequency-stabilizing method.

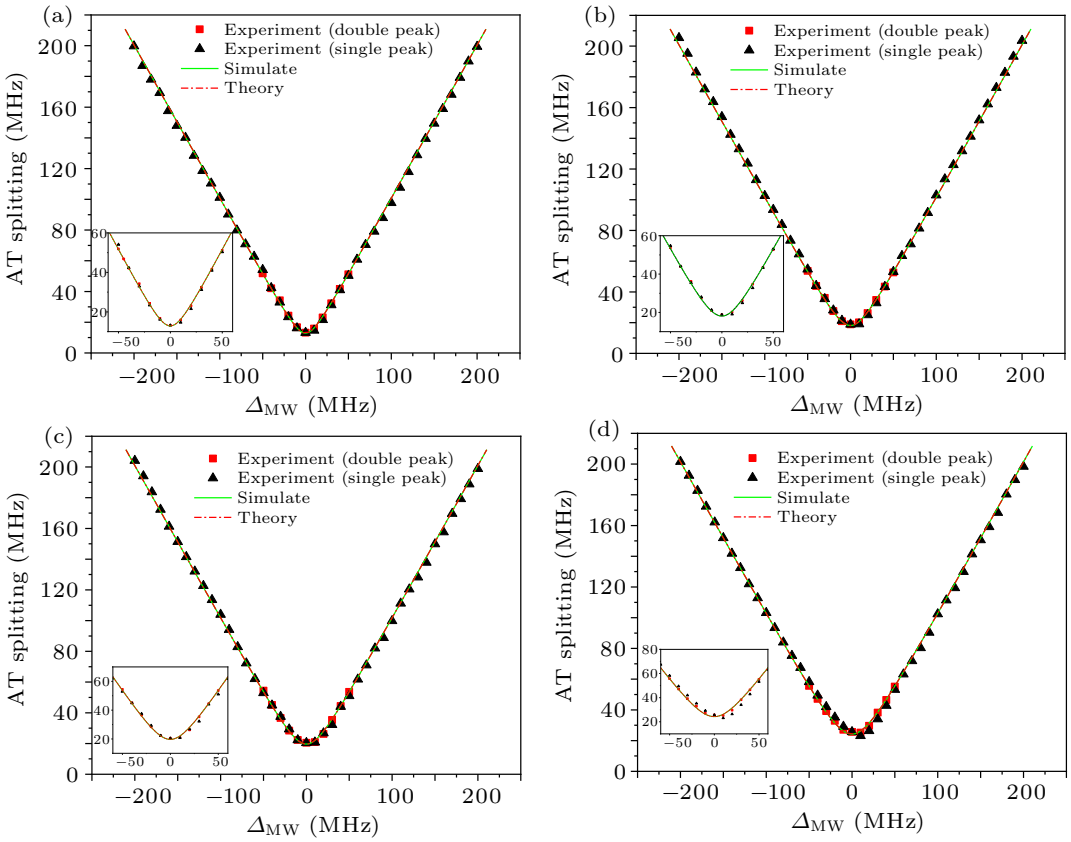



**Fig. 5.** Plots of AT splitting *versus* RF detuning ($\Delta_{\rm MW}$) for power values of signal generator: (a) $-6$ dBm, (b) $-3$ dBm, (c) $-2$ dBm, and (d) 0 dBm, respectively. The red squares represent experimental data obtained by using the standard EIT-AT techniques. The black triangles denote experimental results obtained by using single transmission peak scheme. The green line and red dash line refer to theoretical results, which are generated by simulating this formula $\Omega_{\rm MW,\Delta} = \sqrt{\Omega_{\rm MW}^2 + \Delta_{\rm MW}^2}$ and using the Lindblad master method.

**Table 1.** AT splitting and MW $E$-field strength for different SG power levels.

| Power (dBm) | $\Delta_{\rm MW}$ (MHz) | AT splitting (MHz) | | $E$ (V/m) | |
|---|---|---|---|---|---|
| | | Double peak | Single peak | Double peak | Single peak |
| 0 | 50 | 55.20 | 53.20 | 1.42 | 1.10 |
| | 60 | – | 63.23 | – | 1.21 |
| –2 | 50 | 53.60 | 53.00 | 1.17 | 1.06 |
| | 60 | – | 61.80 | – | 0.90 |
| –3 | 50 | 52.68 | 53.10 | 1.00 | 1.08 |
| | 60 | – | 63.55 | – | 1.27 |
| –6 | 50 | 51.20 | 50.31 | 0.67 | 0.34 |
| | 60 | – | 60.84 | – | 0.61 |

It can be found that the shift of the higher transmission peak decreases as the detuning increases. When the detuning is greater than 200 MHz, the transmission peak shifts less than 0.20 MHz with amplitude increasing in this work, making it difficult to measure. Thus, this method can obtain the results of detuning within 200 MHz. In addition, it should be explicated that the single peak measurement is an effective method when the microwave frequency detuning is known. In recent years, many researchers have investigated the measurement of microwave frequency,[35–38] which is beyound the scope of this work.

## 5. Conclusions

In this work, we proposed a single transmission peak method based on the center of two transmission peaks and the position of the higher transmission peak for measurement of off-resonant MW $E$-field. The center of AT splitting $f_{1/2}$ for the detuned $E$-field is related to the detuning of MW field $\Delta_{\rm MW}$ and central symmetry point $f_0$ of transmission spectrum for the resonant MW field, satisfying the relation $f_{1/2} = \Delta_{\rm MW}/2 + f_0$. The continuous frequencies in a band from $-200$ MHz to $+200$ MHz for power values of signal generator (SG): $-6$ dBm, $-3$ dBm, $-2$ dBm, and 0 dBm, respectively, are detected by using this method, which are in agreement with the theoretical data. The microwave electric field strength can be directly obtained by AT splitting through using this method. At the same time, we also overcome the difficulty that the AT splitting cannot be measured by using the standard EIT-AT techniques[3] and multiple atomic-level Rydberg-atom schemes[26] for the detuning of MW $E$-field frequency 50 MHz $< \Delta_{\rm MW} <$ 200 MHz.

## Data availability statement

The data that support the findings of the present study are openly available in the Science Data Bank at link https://doi.org/10.57760/sciencedb.j00113.00208.

## Acknowledgements

Project supported by the National Key Research and Development Program of China (Grant No. 2021YFF0603704) and the National Natural Science Foundation of China (Grant No. 62071443).

## References

[1] Gallagher T F 1994 *Rydberg Atoms* (Cambridge: Cambridge University Press) pp. 1–9
[2] Bao S, Yang W, Zhang H, Zhang L, Zhao J and Jia S 2015 *J. Phys. Soc. Jpn.* **84** 104301
[3] Sedlacek J A, Schwettmann A, Kübler H, Löw R, Pfau T and Shaffer J P 2012 *Nat. Phys.* **8** 819
[4] Simons M T, Gordon J A, Holloway C L, Anderson D A, Miller S A and Raithel G 2016 *Appl. Phys. Lett.* **108** 174101
[5] Simons M T, Gordon J A and Holloway C L 2016 *J. Appl. Phys.* **120** 123103
[6] Simons M T, Artusio-Glimpse A B, Robinson A K, Prajapati N and Holloway C L 2021 *Measurement: Sensors* **18** 100273
[7] Gordon J A, Holloway C L, Schwarzkopf A, Anderson D A, Miller S, Thaicharoen N and Raithel G 2014 *Appl. Phys. Lett.* **105** 024104
[8] Song Z, Zhang W, Wu Q, Mu H, Liu X, Zhang L and Qu J 2018 *Sensors* **18** 3205
[9] Holloway C L, Simons M T, Gordon J A, Dienstfrey A, Anderson D A and Raithel G 2017 *J. Appl. Phys.* **121** 233106
[10] Jia F D, Liu X B, Mei J, Yu Y H, Zhang H Y, Lin Z Q, Dong H Y, Zhang J, Xie F and Zhong Z P 2021 *Phys. Rev. A* **103** 063113
[11] Mohapatra A K, Jackson T R and Adams C S 2007 *Phys. Rev. Lett.* **98** 113003
[12] Cui Y, Jia F D, Hao J H, Wang Y H, Zhou F, Liu X B, Yu Y H, Mei J, Bai J H, Bao Y Y, Hu D, Wang Y, Liu Y, Zhang J, Xie F and Zhong Z P 2023 *Phys. Rev. A* **107** 043102
[13] Jing M, Hu Y, Ma J, Zhang H, Zhang L, Xiao L and Jia S 2020 *Nat. Phys.* **16** 911
[14] Holloway C L, Gordon J A, Jefferts S, Schwarzkopf A, Anderson D A, Miller S A, Thaicharoen N and Raithel G 2014 *IEEE Trans. Antennas Propag.* **62** 6169
[15] Liao K Y, Tu H T, Yang S Z, Chen C J, Liu X H, Liang J, Zhang X D, Yan H and Zhu S L 2020 *Phys. Rev. A* **101** 053432
[16] Kumar S, Fan H, Kübler H, Sheng J and Shaffer J P 2017 *Sci. Rep.* **7** 42981
[17] Zhou F, Jia F D, Liu X B, Zhang J, Xie F and Zhong Z P 2023 *Acta Phys. Sin.* **72** 045204 (in Chinese)
[18] Downes L A, MacKellar A R, Whiting D J, Bourgenot C, Adams C S and Weatherill K J 2020 *Phys. Rev. X* **10** 011027
[19] Fan H Q, Kumar S, Daschner R, Kübler H and Shaffer J P 2014 *Opt. Lett.* **39** 3030
[20] Song Z, Liu H, Liu X, Zhang W, Zou H, Zhang J and Qu J 2019 *Opt. Express* **27** 8848
[21] Anderson D A, Sapiro R E and Raithel G 2021 *IEEE Trans. Antennas Propag.* **69** 2455

[22] Holloway C, Simons M, Haddab A H, Gordon J A, Anderson D A, Raithel G and Voran S 2021 *IEEE Antennas Propag. Mag.* **63** 63

[23] Meyer D H, Cox K C, Fatemi F K and Kunz P D 2018 *Appl. Phys. Lett.* **112** 211108

[24] Deb A B and Kjærgaard N 2018 *Appl. Phys. Lett.* **112** 211106

[25] Sedlacek J A, Schwettmann A, Kübler H and Shaffer J P 2013 *Phys. Rev. Lett.* **111** 063001

[26] Simons M T, Artusio-Glimpse A B, Holloway C L, Imhof E, Jefferts S R, Wyllie R, Sawyer B C and Walker T G 2021 *Phys. Rev. A* **104** 032824

[27] Liu X H, Liao K Y, Zhang Z X, Tu H T, Bian W, Li Z Q, Zheng S Y, Li H H, Huang W, Yan H and Zhu S L 2022 *Phys. Rev. Appl.* **18** 054003

[28] Calero V, Fernández-Mateo R, Morgan H, García-Sánchez P and Ramos A 2021 *Phys. Rev. Appl.* **15** 014047

[29] Bao S, Zhang H, Zhou J, Zhang L, Zhao J, Xiao L and Jia S 2016 *Phys. Rev. A* **94** 043822

[30] Kwak H M, Jeong T, Lee Y S and Moon H S 2016 *Opt. Commun.* **380** 168

[31] Thaicharoen N, Moore K R, Anderson D A, Powel R C, Peterson E and Raithel G 2019 *Phys. Rev. A* **100** 054003

[32] Steck D A 2013 *Rubidium* 87*D Line Data* available online: https://steck.us/alkalidata

[33] Fleischhauer M, Imamoglu A and Marangos J P 2005 *Rev. Mod. Phys.* **77** 633

[34] Ibali N, Pritchard J D, Adams C S and Weatherill K J 2017 *Comput. Phys. Commun.* **220** 319

[35] Liu J, Shi T and Chen Y 2021 *J. Lightwave Technol.* **39** 2023

[36] Dai Z J, Chen X, Wang P, Zhang J and Liang H J 2023 *Journal of China Academy of Electronics and Information Technology* **18** 455 (in Chinese)

[37] Zhang X Y, Liang T and An K 2023 *J. Microwaves* **39** 7 (in Chinese)

[38] Zhang S T 2013 *The Research of Microwave Frequency Based on Photonics Methods* (Dalian University of Technology) (in Chinese)